Journal of Alloys and Compounds 509 (2011) 9183–9189

Contents lists available at ScienceDirect

Journal of Alloys and Compounds

journal homepage: www.elsevier.com/locate/jallcom

Characterization of cobalt oxide thin films prepared by a facile spray pyrolysis technique using perfume atomizer

A. Louardi, A. Rmili, F. Ouachtari, A. Bouaoud, B. Elidrissi*, H. Erguig

Laboratoire des Hautes Energies, Sciences de l'Ingénierie et Réacteurs (LHESIR), Equipe Ingénierie et Matériaux (INMA), Département de Physique, Faculté des Sciences, Kénitra, Morocco

ARTICLE INFO

Article history:
Received 5 April 2011
Received in revised form 24 June 2011
Accepted 27 June 2011
Available online 18 July 2011

Keywords:
Cobalt oxide
Spray pyrolysis
Thin film
Morphology
Raman spectroscopy
Optical properties

ABSTRACT

Cobalt oxide (Co_3O_4) thin films were prepared by a facile spray pyrolysis technique using perfume atomizer from aqueous solution of hydrated cobalt chloride salt ($CoCl_2{\cdot}6H_2O$) as source of cobalt. The films were deposited onto the amorphous glass substrates kept at different temperatures (300–500 °C). The influences of molar concentration of the starting solution and substrate temperature on the structural, morphological and optical properties of (Co_3O_4) thin films were studied. It was found from X-ray diffraction (XRD) analysis that the films prepared with molar concentration greater than 0.025 M/L were polycrystalline spinel type cubic structure. The preferred orientation of the crystallites of these films changes gradually from (6 2 2) to (1 1 1) when the substrate temperature increases. By Raman spectroscopy, five Raman active modes characteristic of Co_3O_4 spinel type cubic structure were found and identified at 194, 484, 522, 620 and 691 cm^{-1}. The scanning electron microscopy (SEM) images showed micro porous structure with very fine grains less than 50 nm in diameter. These films exhibited also a transmittance value of about 70% in the visible and infra red range.

1. Introduction

Cobalt oxide thin films have attracted substantial research effort in recent years because their potential application in various technological areas. They can be used as high temperature solar selective absorbers [1], electrochemical capacitors [2], optical gas sensors [3], heterogeneous catalysts [4], anodic electrochromic materials in smart window devices [5], negative electrodes in lithium-ion batteries [6] and magnetic materials [7]. In general, cobalt oxide exists in three different crystalline forms; namely CoO, Co_2O_3 and Co_3O_4 [8], but the latter stoichiometry is largely reported for the above cited applications because of its chemical stability and desired electrochemical properties. Co_3O_4 thin films were prepared by employing different techniques such as R-F magnetron sputtering [9], atomic layer deposition [10], chemical vapour deposition [11], sol–gel process [12], co-precipitation method [13], pulsed laser deposition [14] chemical bath deposition [15] and spray pyrolysis [16]. Among these deposition techniques, spray pyrolysis has several advantages: its low cost, flexibility, capability for preparing porous and nanostructure thin films and convenient for large area deposition. This technique has been used successfully in our laboratory to fabricate a variety of porous materials for electrochromic devices such as WO_3, [17], Fe_2O_3 [18], and CeO_2 [19].

It is well shown that the porous structure is highly desired to ameliorate the electrochemical properties of electrochromic materials as well as catalysts such as cobalt oxide (Co_3O_4). Thus, controlling the morphology of cobalt oxide thin films is very important. In the present work, we have studied, for the first time, the effect of substrate temperature and molar concentration of the starting solution on the structure, morphology and optical properties of the cobalt oxide thin films elaborated by a simplified spray pyrolysis technique using perfume atomizer.

2. Experimental procedures

2.1. Preparations of thin films by spray pyrolysis using a perfume atomizer

Cobalt oxide thin films were prepared from solution of hydrated cobalt chloride $CoCl_2{\cdot}6H_2O$ dissolved in 50 ml of deionized water, stirred thoroughly using a magnetic stirrer for 20 min and then sprayed manually in fine droplets using a perfume atomizer on the pre-heated glass substrates kept at different temperatures. Before the deposition process, the glass substrates were degreased with organic solvent, rinsed with deionised water and dried in air. The spray pyrolysis method using a perfume atomizer has been successfully used by Sawada et al. [20] and Fukano et al. [21] for the deposition of tin oxide (SnO_2), and Ravichandran and Philominathan [22] for the deposition of cadmium sulfide (CdS).

2.2. Characterization

The as deposited films were black in colour and found to be uniform, pin holes-free and strongly adherent to the glass substrates. Their thickness was calculated

---

* Corresponding author. Tel.: +212 7372770.
E-mail address: e.bachir@mailcity.com (B. Elidrissi).

0925-8388/$ – see front matter © 2011 Elsevier B.V. All rights reserved.
doi:10.1016/j.jallcom.2011.06.106

by using gravimetric method and it was found to vary from 400 to 500 nm. The structure, crystallinity and phase of the Co_3O_4 thin films were determined by the X-ray diffraction (XRD) analysis, using Cu Kα radiation with 2θ ranging from 15° to 80° and Raman spectroscopy using FT-RAM II spectrometer. The Raman spectra were obtained from 100 to 1200 cm^{-1}, using Nd: YAG laser ($\lambda = 1064$ nm) as excitation source. The surface morphology of the films was characterized by scanning electron microscopy (SEM). In order to determine the band gap energy of Co_3O_4 in thin film form, the optical transmission studies were carried out in the wavelength range of 300–2500 nm, using a SHIMADZU 3101 PC UV-VIS-NIR spectrophotometer.

3. Results and discussion

3.1. Crystal structure determination

Fig. 1 shows the X-ray diffraction diagrams of the cobalt oxide thin films elaborated by using a perfume atomizer. It is seen that the films prepared from solutions having molar concentration of $CoCl_2{\cdot}6H_2O$ equal to 0.01 M/L do not display any diffraction peaks, probably because these films have low thicknesses. The films prepared from solutions having molar concentration of $CoCl_2{\cdot}6H_2O$ greater than 0.025 M/L show multiple diffraction peaks at $2\theta = 18.9°$, 31.3°, 36.9°, 44.9°, 59.5° and 79.02° indicating the polycrystalline nature of these films. The interplanar spacing values corresponding to the (1 1 1), (2 2 0), (3 1 1), (2 2 2), (4 0 0), (5 1 1), (4 4 0), and (6 2 2) diffraction planes are compared with the standard values of Co_3O_4 [23]. A matching of the calculated d_{hkl} values and the standard ones confirms that the deposited films are crystallized in the spinel type cubic structure of Co_3O_4 (Fd3m space group) with a preferential orientation along the [1 1 1] direction. However, Hamdani et al. [24] and Avila et al. [25] have found [3 1 1] as a preferred orientation for their films of Co_3O_4 obtained by using spray pyrolysis technique. Moreover, no peaks from other cobalt oxides like CoO or Co_2O_3 are detected, suggesting that Co_3O_4 is more stable. The lattice parameter a of the unit cell is calculated from the peak positions using the formula of cubic system.

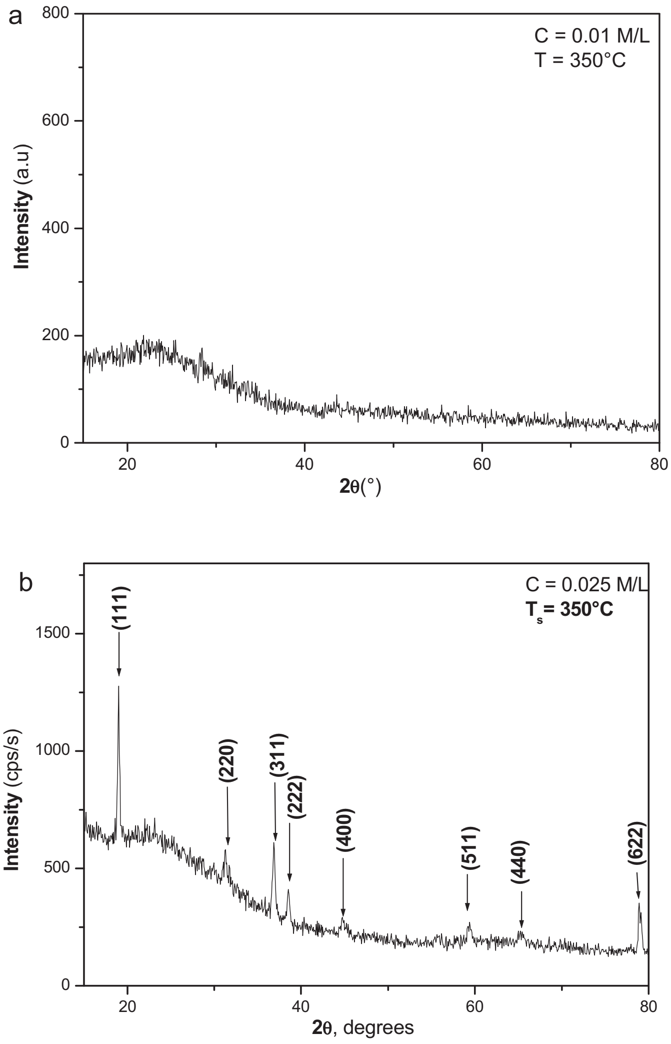

Fig. 1. X-ray diffraction patterns of Co_3O_4 thin films prepared with different molar concentrations of $CoCl_2{\cdot}6H_2O$ solution: (a) 0.01 M/L and (b) 0.03 M/L.

$$d_{h\,k\,l} = \frac{a}{\sqrt{(h^2 + k^2 + l^2)}} \qquad (1)$$

The value is found to be $a = 8.045$ Å, which is close to that given by JCPDS 42-1467 ($a = 8.084$ Å) [23].

Fig. 2 shows the diffraction patterns of Co_3O_4 thin films prepared at substrate temperature varying from 300 to 500 °C. This figure indicates that all the deposited films are polycrystalline and exhibit the single phase Co_3O_4 spinel type cubic structure. It shows also that the whole X-ray diffraction diagrams exhibit a broad hump located at around $2\theta = 22°$, which is due to the glass substrates. Furthermore, with the increase of substrate temperature the crystallinity of the Co_3O_4 thin films improves and the preferred orientation of the crystallites changes gradually from [6 2 2] to [1 1 1] direction. However, the crystallinity and [1 1 1] orientation degrades at higher substrate temperature ($T_s = 500$ °C). Higher substrate temperature is favourable for the diffusion of atoms adsorbed on the substrate and accelerates the migration of atoms for energetically favourable positions, resulting in the enhancement of crystallinity and [1 1 1] orientation of the films. However at excessively high substrate temperature ($T_s = 500$ °C), some droplets have been decomposed to Co_3O_4 particles before reaching substrate. The preferred orientation of the Co_3O_4 thin films is evaluated by the texture coefficient (TC), calculated from the X-ray data using the well-known formula:

$$\mathrm{TC}(h\;k\,l) = \frac{I(h\,k\,l)/I_0(h\,k\,l)}{1/N\sum_{h\,k\,l} I(h\,k\,l)/I_0(h\,k\,l)} \qquad (2)$$

where TC($h\,k\,l$) is the texture coefficient of the $h\,k\,l$ planes, I is the measured or normalized intensity, I_0 the corresponding standard intensity given in JCPDS data, and N the number of reflections. The preferred orientation of a film will be ($h\,k\,l$) plane for the higher value of TC($h\,k\,l$). Fig. 3 presents TC($h\,k\,l$) values calculated from the above equation for the reflections (1 1 1) and (6 2 2) of the cubic Co_3O_4 at the examined substrate temperature range. It is observed that at substrate temperature equal to 400 °C the (1 1 1) peak has the highest texture coefficient. The (1 1 1) preferred orientation can maybe explained by the tendency of minimization of surface energy of films deposited on glass substrate. The average crystallite size ($D_{h\,k\,l}$) of the Co_3O_4 thin films are estimated from the X-ray diffraction patterns using the Scherrer formula [26]:

$$D_{h\,k\,l} = 0.9\frac{\lambda}{\beta_{h\,k\,l}\cos(\theta_{h\,k\,l})} \qquad (3)$$

where λ is the wavelength of incident radiation ($\lambda = 1.544$ Å), $\beta_{h\,k\,l}$ is the full-width at half maximum (FWHM) of the preferential orientation diffraction peak and $\theta_{h\,k\,l}$ is the Bragg diffraction angle. The calculated values are reported in Table 1. As it can be seen the values are found to be varied between 31 and 40 nm as the substrate

Table 1
Average crystallite size of the Co_3O_4 thin films prepared at different substrate temperatures.

Temperature (°C)	300 °C	350 °C	400 °C	500 °C
Crystallite size (nm)	32 ± 6	40 ± 8	31 ± 6	30 ± 6

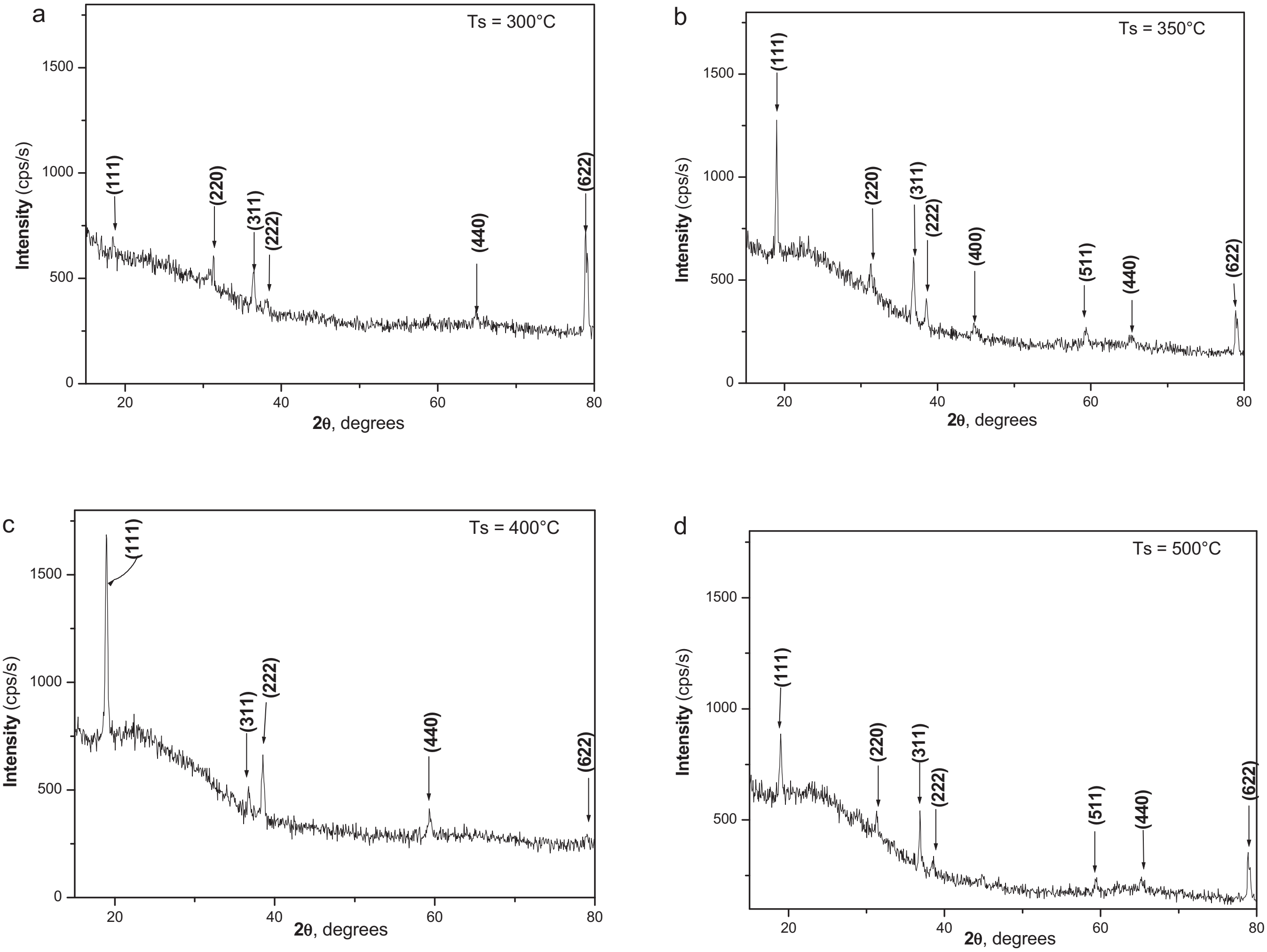

Fig. 2. X-ray diffraction patterns of Co_3O_4 thin films deposited at different substrate temperatures: (a) 300 °C, (b) 350 °C, (c) 400 °C and (d) 500 °C.

temperature changed from 300 to 500 °C, suggesting the formation of nanostrucrured polycrystalline Co_3O_4 thin film. Besides, the film prepared at $T_s = 350\,^\circ C$ has sharper (1 1 1) diffraction peak and larger crystallite size about (40 nm) than the films prepared at 300, 400 and 500 °C, suggesting a better crystallinity for the film prepared at this temperature ($T_s = 350^\circ$).

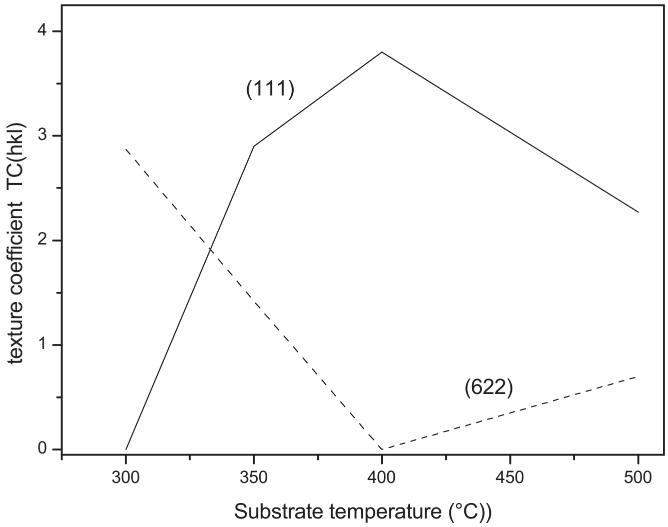

Fig. 3. Variation of TC(*hk*) values with substrate temperature: (a) TC(1 1 1), (b) TC(6 2 2).

3.2. Surface morphology

The influence of substrate temperature on the surface morphology of the spray deposited Co_3O_4 thin films is studied by scanning electron microscopy. Fig. 4(a)–(d) shows the SEM images of Co_3O_4 thin films prepared at 300, 350, 400 and 500 °C at low magnification (20,000×), It is clearly seen that the films have an heterogeneous surfaces with porous structure. Coalescence of smaller grains of different sizes and shapes into bigger ones can be noticed when the substrate temperature increases. Fig. 5 shows the SEM images of Co_3O_4 thin films prepared at 300 °C at high magnification (160,000×). The image shows a microporous structure with very fine spherical grains less than 50 nm in diameter, confirming the X-ray diffraction results.

3.3. Raman spectroscopy

Raman spectroscopy is used to determine the structure, crystallinity and phases of our thin films. The Co_3O_4 oxide crystallises in the normal spinel structure, in which the Co^{2+} ions occupy the 8a sites and Co^{3+} ions occupy the octahedral 16d sites. From the group theory, this structure has five Raman active modes, which are $F^3{}_{2g}$, E_g, $F^1{}_{2g}$, $F^2{}_{2g}$ and A_{1g}. Fig. 6(a)–(d) shows Raman spec-

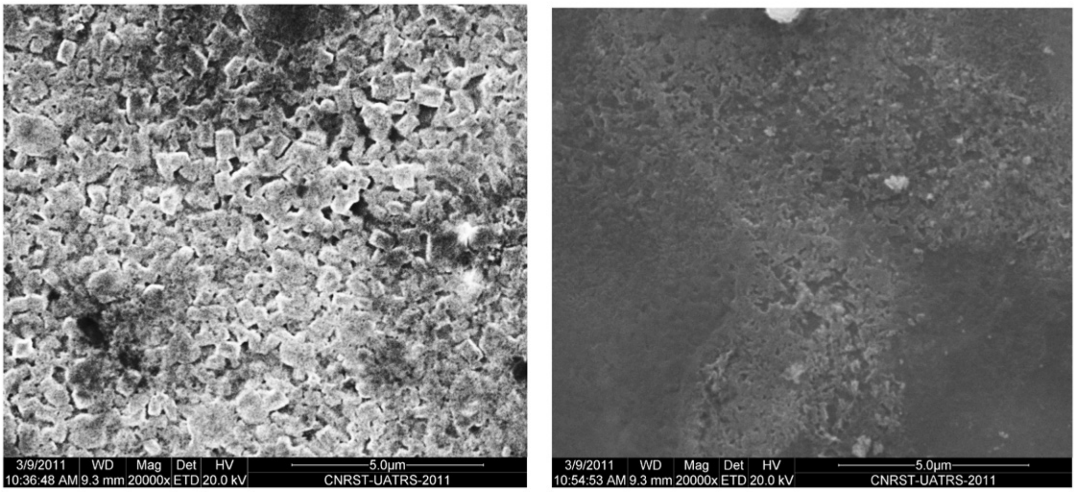

(a) : T = 300°C (20000x) (b) : T= 350°C (20000x)

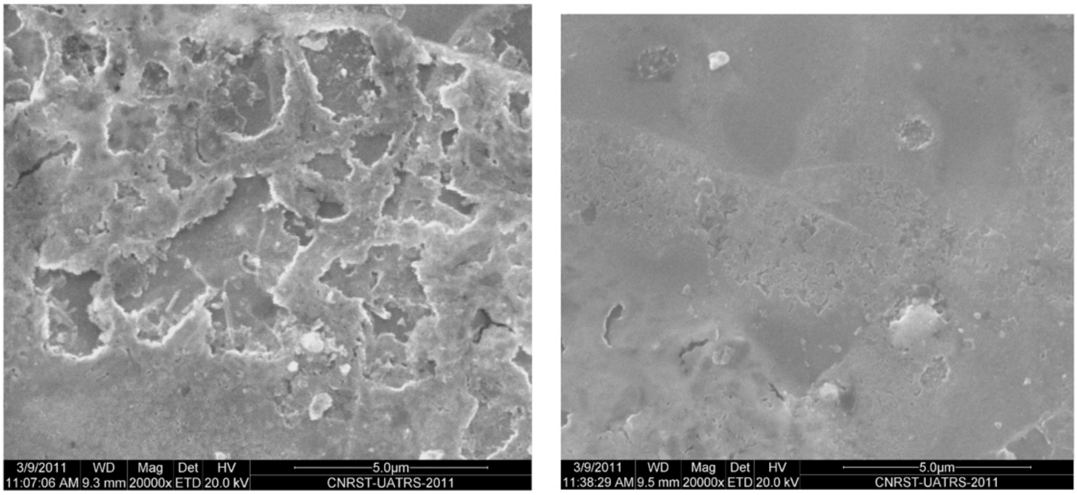

(c) : T = 400°C (20000x) (d) : T = 500°C (20000x)

Fig. 4. SEM micrographs (20,000×) of Co_3O_4 thin films deposited at different substrate temperatures: (a) 300 °C, (b) 300 °C, (c) 400 °C and (d) 500 °C.

tra of cobalt oxide thin films prepared at substrate temperature between 300 and 500 °C. As it can be observed all the deposited films show five well-defined Raman peaks located at 197, 484, 523, 621 and 691 cm^{-1}, which correspond, respectively to $F^3{}_{2g}$, E_g, $F^1{}_{2g}$, $F^2{}_{2g}$ and A_{1g} modes of crystalline Co_3O_4, in agreement with the group theory. Beside the five Raman peaks of Co_3O_4, there are two broad peaks located at 559 and 1094 cm^{-1}, which are attributed to Si–O vibration modes of SiO_2 glass substrate. Moreover, no Raman peaks of CoO and Co_2O_3 are detected, in particular the Raman peaks of CoO located at 484 and 691 cm^{-1} [27]. This indicates that the as prepared films consist of a single phase (Co_3O_4), confirming the X-ray diffraction measurements. Fig. 6(a)–(d) shows also that all the Raman peaks became sharper and more intense when the substrate temperature increases up to 350 °C. As the substrate temperature increases beyond 350 °C, the Raman peaks became wider and less intense indicating a deterioration of the films crystallinity that lead to a decrease of the crystal dimensions of the films as it is found by X-ray diffraction analysis and scanning electron microscopy (Table 1). Fig. 7 shows the full width at half maximum (FWHM) values of the Raman peak A_{1g} (691 cm^{-1}) of Co_3O_4 thin films with substrate temperature. As it can be seen, the film prepared at 350 °C exhibits relatively narrow Raman peak and higher Raman intensity. This indicates that the film prepared at T_s = 350 °C has a better crystallinity than those obtained at 300, 400 and 500 °C, confirming the X-ray diffraction results.

3.4. Optical properties

The optical properties such as transmittance, absorption coefficient and band gap energy of Co_3O_4 thin films are determined from the variation of the optical transmission with wavelength (λ) in the range of 300–1500 nm. As the examination is done for the film–substrate combination, the transmission of the substrates is also measured and subtracted. Fig. 8 shows plots of optical transmission of the Co_3O_4 thin films deposited at substrate temperature of 300 and 500 °C. It can be seen that the optical transmission improves when the substrate temperature increases. The film deposited at higher substrate temperature (T_s = 500 °C) shows an average optical transmittance of about 70% in the visible and near infrared region. This is can be explained by a less light scattering of this film due to its smoothest surface and relatively a better crystallinity than that prepared at 300 °C. Fig. 8 shows also two

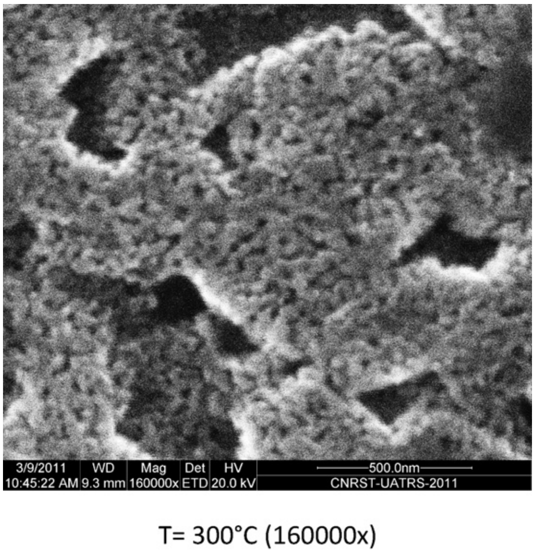

Fig. 5. SEM image of Co_3O_4 thin film deposited at substrate temperature of 300 °C at high magnification (160,000×).

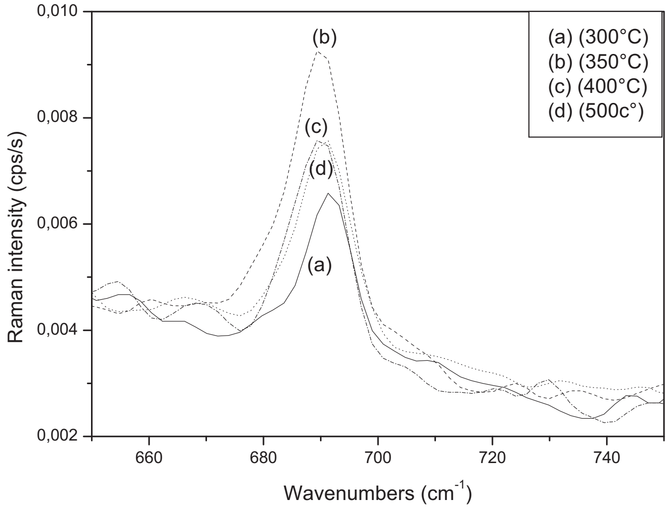

Fig. 7. The full width at half maximum (FWHM) of the Raman peak E_g (484 cm^{-1}) of Co_3O_4 thin films prepared at: (a) 300 °C, (b) 350 °C, (c) 400 °C and (d) 500 °C.

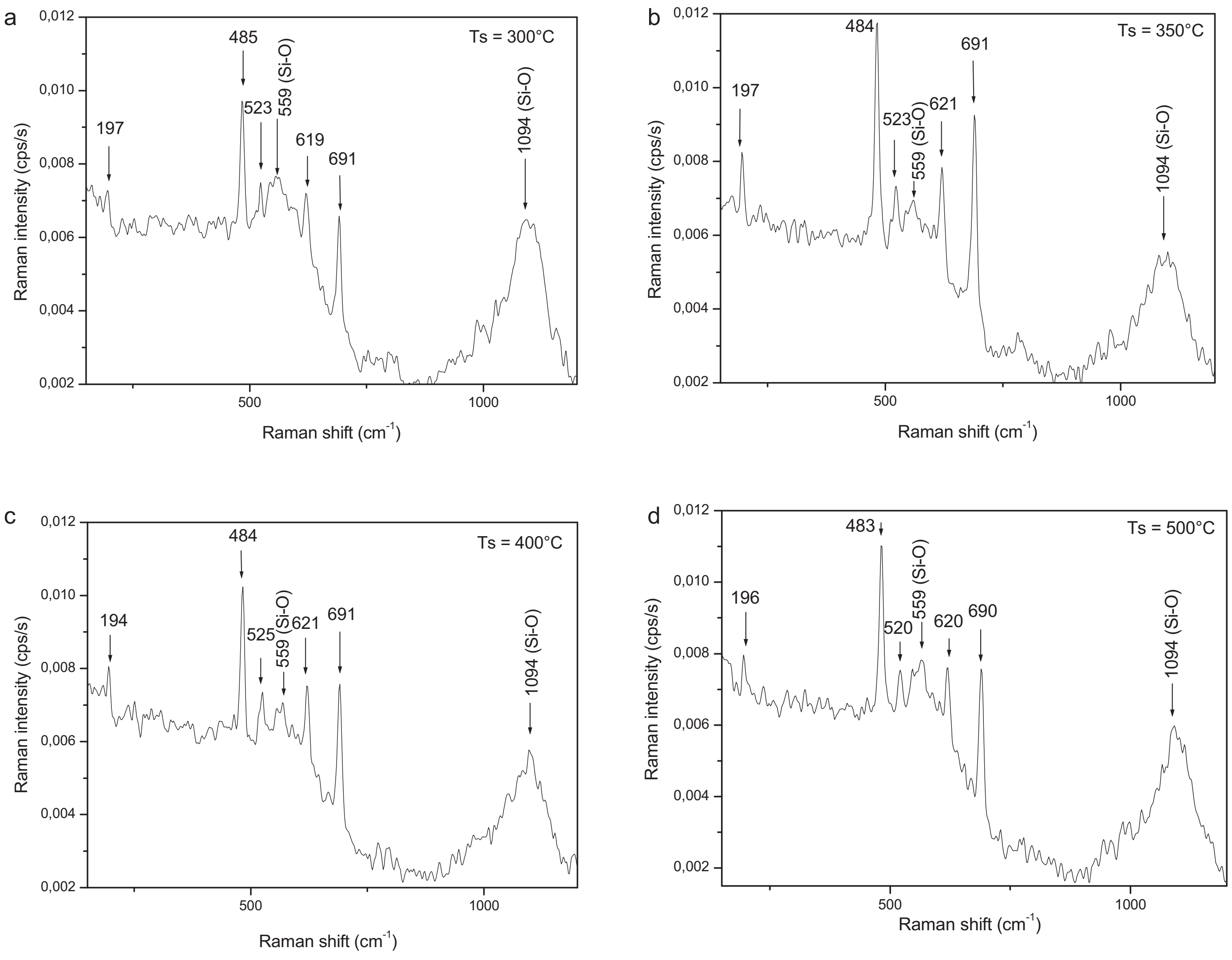

Fig. 6. Raman spectra of cobalt oxide thin films prepared at different substrate temperatures: (a) 300 °C, (b) 350 °C, (c) 400 °C and (d) 500 °C.

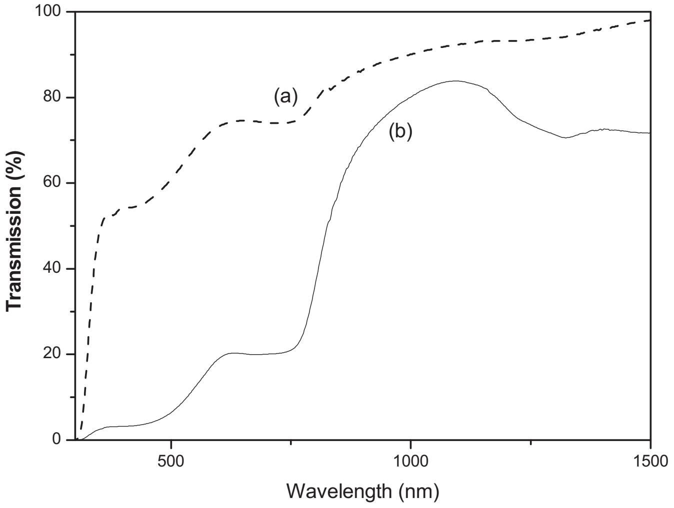

Fig. 8. Transmission spectra of Co_3O_4 thin films deposited at: (a) 300 °C and (b) 500 °C.

sharp absorption edges in the visible region. This indicates that the absorption band gap transitions in the Co_3O_4 thin films are direct. From the solid band theory, the relationship between the absorption coefficient α and the energy of the incident light $h\upsilon$ near the absorption edge of semiconductors is given by the Tauc's relation:

$$(\alpha \ h\nu) = A(h\nu - E_g)^n \tag{4}$$

where A is a constant, E_g the band gap energy and n a constant equal to 0.5, 2, 1.5 and 3 for allowed direct, allowed indirect, forbidden direct and forbidden indirect transitions, respectively. Fig. 9(a) and (b) shows the plots of $(\alpha h\nu)^2$ versus $(h\nu)$ for Co_3O_4 thin films prepared at T_s = 300 and 500 °C, respectively. Two straight line portions have been observed, indicating the existence of two direct band gap values of cobalt oxide in agreement with the literature [28]. The band gaps (E_g) of the deposited films are in the range 1.48–1.51 eV for lower energy side region and 2.08–2.11 eV for higher energy side region, which are consistent with the reported Co_3O_4 band structure [29–31]. It can be seen also that the E_g value varies slightly with substrate temperature. This little shift may be attributed to the changes of the quality of the Co_3O_4 films with increasing substrate temperature.

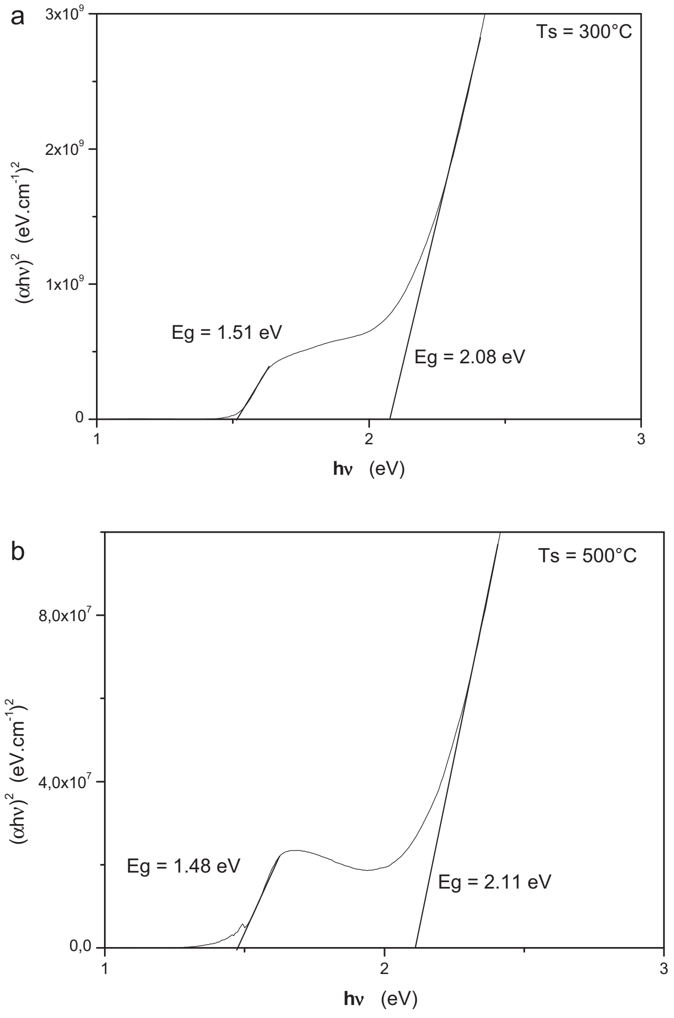

Fig. 9. Plots of $(\alpha h\nu)^2$ against $h\nu$ of Co_3O_4 thin films prepared at: 300 °C and (b) 500 °C.

4. Conclusions

Cobalt oxide (Co_3O_4) thin films were prepared by a facile spray pyrolysis technique using perfume atomizer from aqueous solution of hydrated cobalt chloride ($CoCl_2{\cdot}6H_2O$) as source of cobalt. The structural, morphological and optical properties of them were investigated as function of molar concentration and substrate temperature. It is shown that the films deposited with molar concentration of cobalt chloride in the solution greater than 0.025 M/L at substrate temperatures varied from 300 to 500 °C were polycrystalline spinel type cubic structure. Five Raman peaks located at 197, 484, 523, 621 and 691 cm^{-1}, which are characteristic of Co_3O_4 films, were detected in agreement with the group theory. SEM images reveal that these films have micro porous structure with very fine spherical grains less than 50 nm in diameter. These films exhibited also a transmittance value of about 70% in the visible and infra red range. This makes Co_3O_4 thin films a promising material for using as electrochromic material in smart windows devices.

References

[1] E. Barrera, L. Huerta, S. Muhl, A. Avila, Sol. Energy Mater. Sol. Cells 88 (2005) 179–186.
[2] Y. Li, K. Huang, Z. Yao, S. Liu, X. Qing, Electrochem. Acta 56 (2011) 2140–2144.
[3] X. Liu, G. Qiu, X. Li, Nanotechnology 16 (2005) 3035.
[4] X.W. Xie, Y. Li, Z.Q. Liu, M. Haruta, W.J. Shen, Nature 458 (2009) 746.
[5] X.H. Xia, J.P. Tu, J. Zhang, X.H. Huang, X.L. Wang, W.K. Zhang, H. Huang, Electrochem. Commun. 10 (2008) 1815–1818.
[6] K.M. Shaju, F. Jiao, A. Debart, P.G. Bruce, Phys. Chem. Chem. Phys. 9 (2007) 1837.
[7] N.R. Jana, Y.F. Chen, X.G. Peng, Chem. Mater. 16 (2004) 3931.
[8] S.G. Kandalkar, C.D. Lokande, R.S. Mane, S.H. Hun, Appl. Surf. Sci. 253 (2007) 3952.
[9] C.L. Liao, Y.H. Lee, S.T. Chang, K.Z. Fuang, J. Power Sources 158 (2006) 1379–1385.
[10] K.B. Klepper, O. Nilson, H. Fjellvag, J. Cryst. Growth 307 (2007) 457–465.
[11] N. Bahlawane, E.F. Rivera, K.K. Honghaus, A. Brechling, U. Kleinberg, Appl. Catal. B 53 (2004) 245–255.
[12] F. Svegl, B. Orel, I.G. Svegl, V. Kaucic, Electrochem. Acta 45 (2000) 4359–4371.
[13] J. Pal, P. Chauhan, Mater. Charact. 61 (2010) 575–579.
[14] S.-L. Chou, J.Z. Wang, H.K. Liu, S.H. Dou, J. Power Sources 182 (2008) 359–364.
[15] Z.W. Fu, Y. Wang, Y. Zhang, Q.Z. Qin, Solid State Ionics 170 (2004) 105–109.
[16] L.D. Kadam, S.H. Pawar, P.S. Patil, Mater. Chem. Phys. 68 (2001) 280–282.
[17] M. Regragui, M. Addou, A. Outzourhit, J.C. Bernède, B. Elidrissi, E. Benseddik, A. Kachouane, Thin Solid Films 358 (2000) 40–45.
[18] L. Dghoughi, B. Elidrissi, M. Addou, J.C. Bernède, M. Regragui, M. Alaoui Lamrani, H. Erguig, Appl. Surf. Sci. 253 (2006) 1823–1829.
[19] B. Elidrissi, M. Addou, M. Regragui, C. Monty, A. Bougrine, A. Kachouane, Thin Solid Films 379 (2000) 23–27.
[20] Y. Sawada, C. Kobayashi, S. Seki, H. Funakibo, Thin Solid Films 409 (2002) 46–50.
[21] T. Fukano, T. Motohiro, Sol. Energy Mater. Sol. Cells 82 (2004) 567–575.

[22] K. Ravichandran, P. Philominathan, Solar Energy 82 (2008) 1062–1068.
[23] Standard JCPDS Data Card, JCPDS 42-1467.
[24] M. Hamdani, J.F. Koening, P. Chartier, J. Appl. Electrochem. 18 (1988) 561–567.
[25] G.A. Avila, et al., Sol. Energy Mater. Sol. Cells 82 (2004) 269–278.
[26] B.D. Cullity, S.R. Stock, Elements of X-ray Diffraction , Prentice-Hall, Pearson, 2001.
[27] D. Gallant, M. Pézolet, S. Simard, J. Phys. Chem. B 110 (2006) 6871–6880.
[28] A. Gulino, G. Fiorito, I. Fragala, J. Mater. Chem. 13 (2003) 861–865.
[29] T. Maruyama, T. Nakai, Sol. Energy Mater. Sol. Cells 23 (1991) 25.
[30] P.S. Patil, L.D. Kadam, C.D. Lokhande, Thin Solid Films 272 (1996) 29.
[31] D. Barreca, C. Massignan, S. Daolio, M. Fabrizio, C. Picirillo, L. Armelao, E. Tondello, Chem. Mater. 13 (2001) 588.